Supporting Information

Surfactant stabilization of vanadium iron oxide derived from Prussian blue analog for lithium-ion battery electrodes

Behnoosh Bornamehr[1,2], Hiba El Gaidi[1,2],

Stefanie Arnold[1,2], Emmanuel Pameté[1], Volker Presser[1,2,3,*]

[1] *INM – Leibniz Institute for New Materials, Campus D2 2, 66123, Saarbrücken, Germany*

[2] *Department of Materials Science & Engineering, Saarland University, Campus D2 2, 66123, Saarbrücken, Germany*

[3] *Saarene – Saarland Center for Energy Materials and Sustainability, Campus C4 2, 66123 Saarbrücken, Germany*

* Corresponding author: volker.presser@leibniz-inm.de (VP)

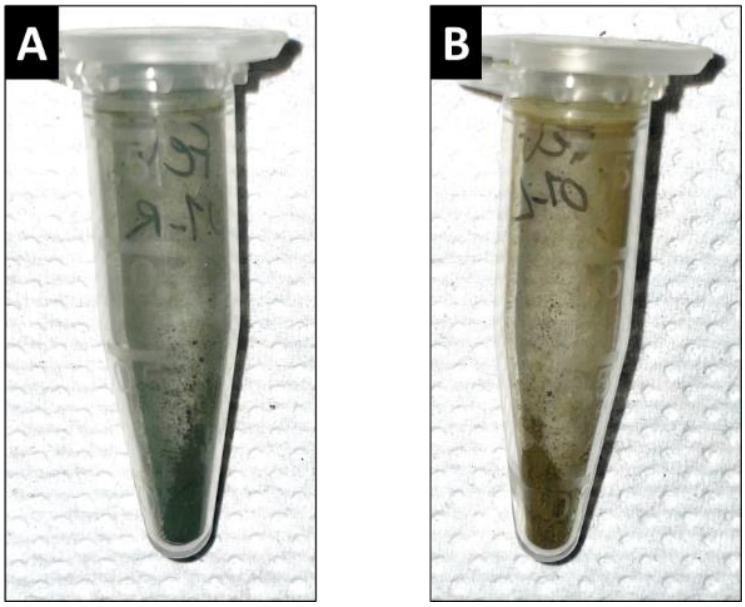

Figure S1. Photographs of FeV oxidation under synthetic air resulting in inhomogeneous oxide formation at **A** low stream and **B** upstream of the furnace.

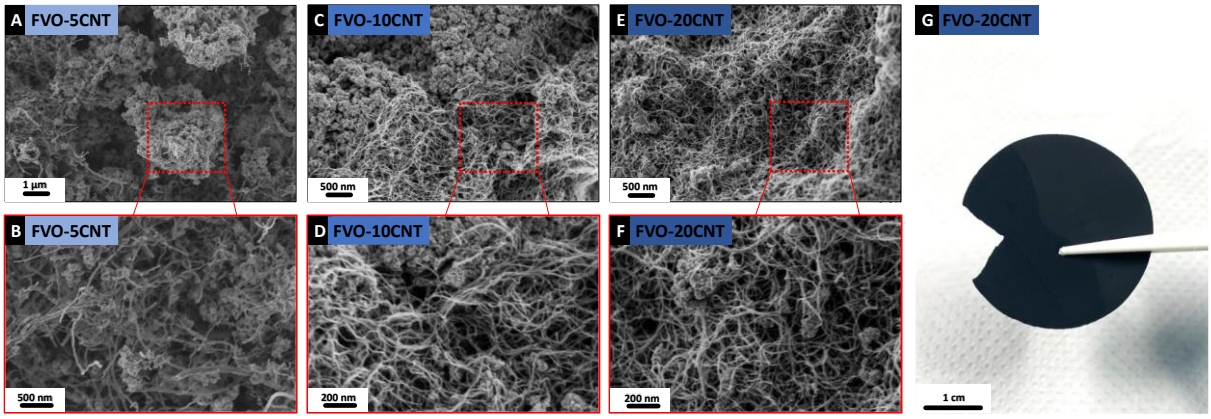

Figure S2. A-F Scanning electron micrographs of FVO mixed with different mass ratios (5, 10, 20 mass%) of CNT. **G** Photograph of the filtrated self-standing FVO on CNTs used for cutting the electrodes.

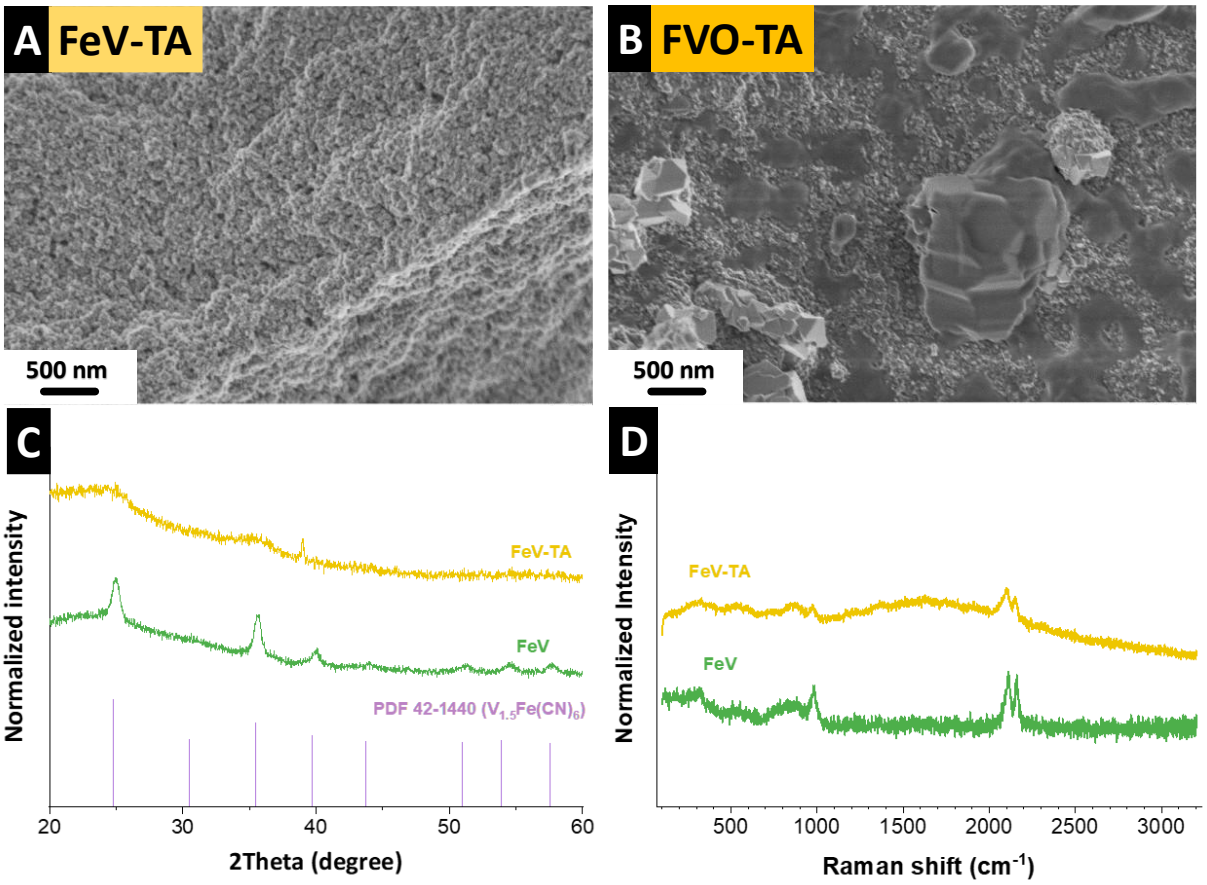

Figure S3. Scanning electron micrographs of **A** FeV synthesized with tannic acid and **B** its resulting oxide. **C** Respective X-ray diffractograms and **D** Raman spectra.

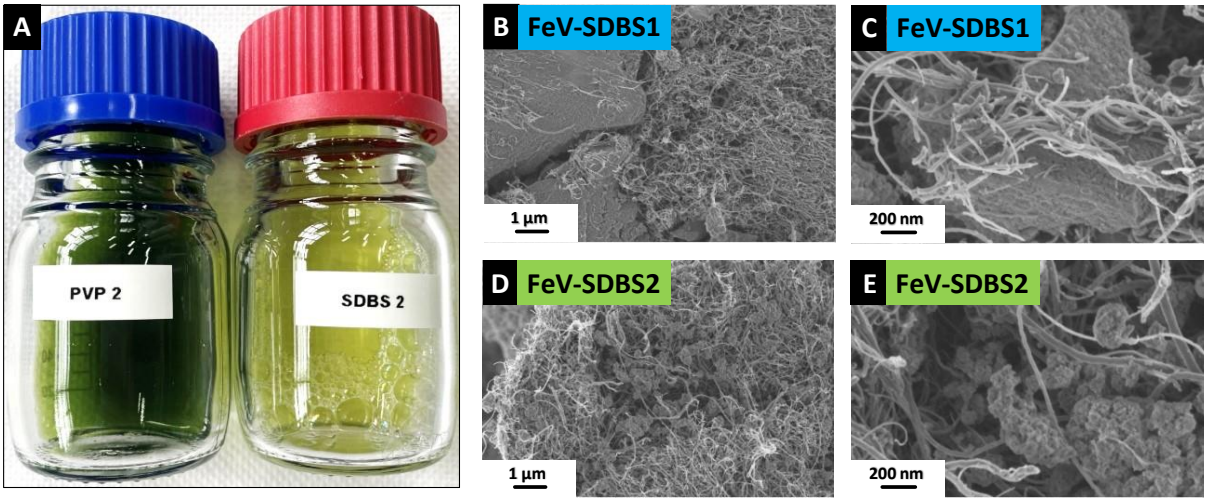

Figure S4. A Photograph of the residual supernatants after centrifugation of PVP and SDBS containing synthesis solutions. **B-C** Scanning electron micrographs of FeV-SDBS1 and **D-E** of FeV-SDBS2.

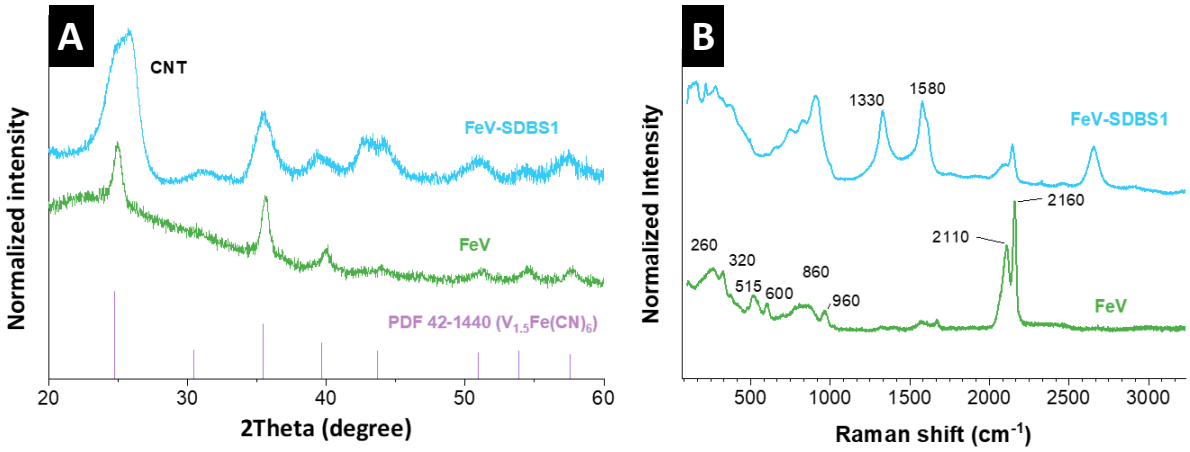

Figure S5. A X-ray diffractograms and **B** Raman spectrum of FeV-SDBS1 compared to the FeV.

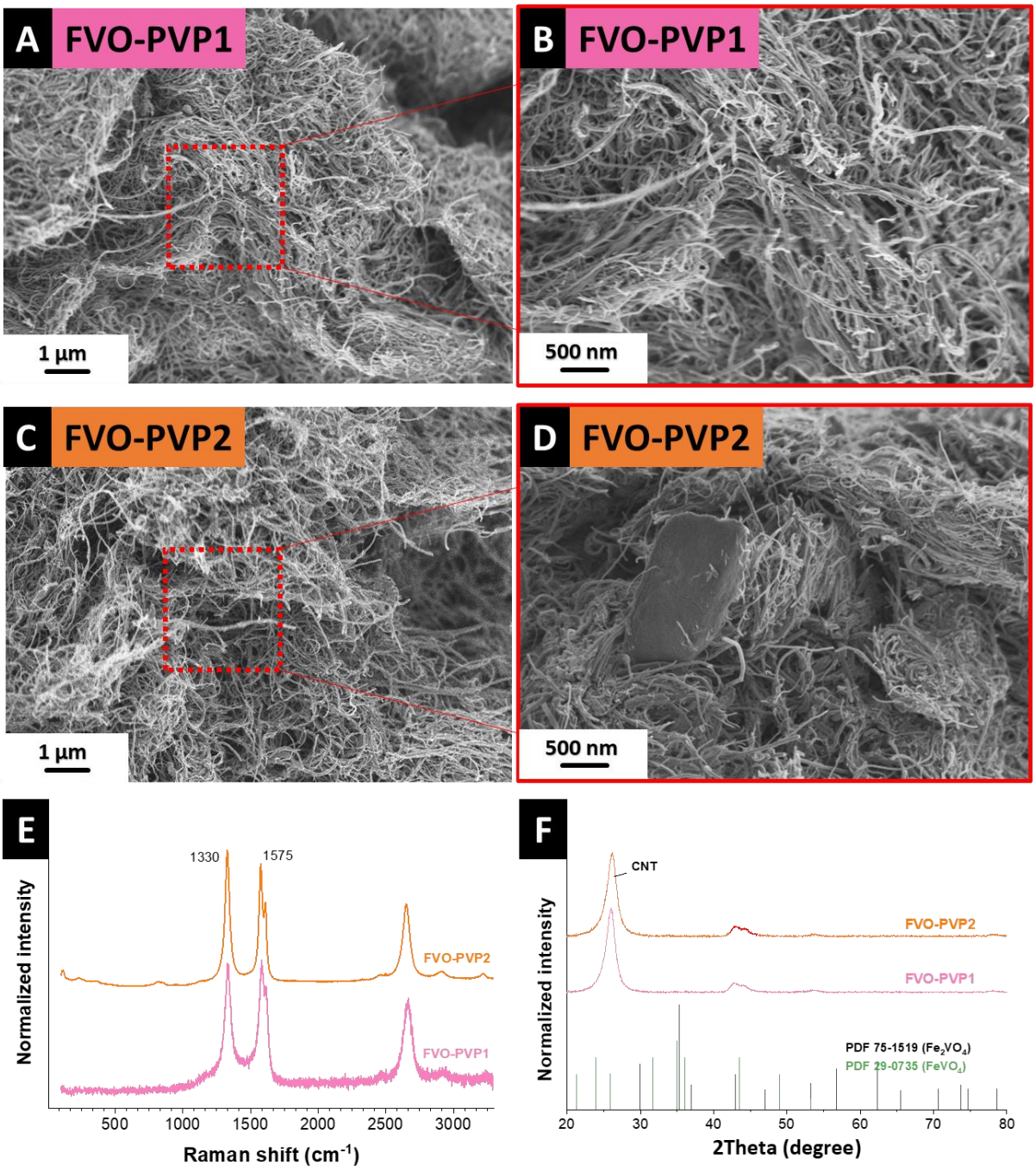

Figure S6. Scanning electron micrographs of **A-B** FeV-PVP1 and **C-D** FeV-PVP2 and their respective **E** Raman spectra and **F** X-ray diffractograms.

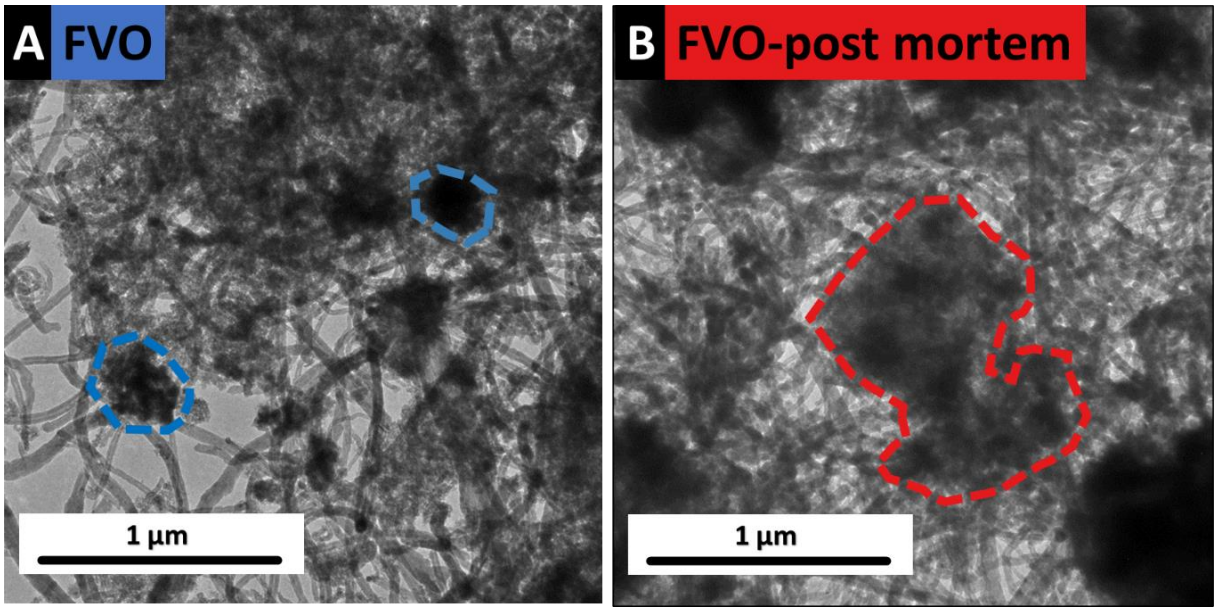

Figure S7. Transmission electron micrographs of the FVO electrode **A** before and **B** after cycling.

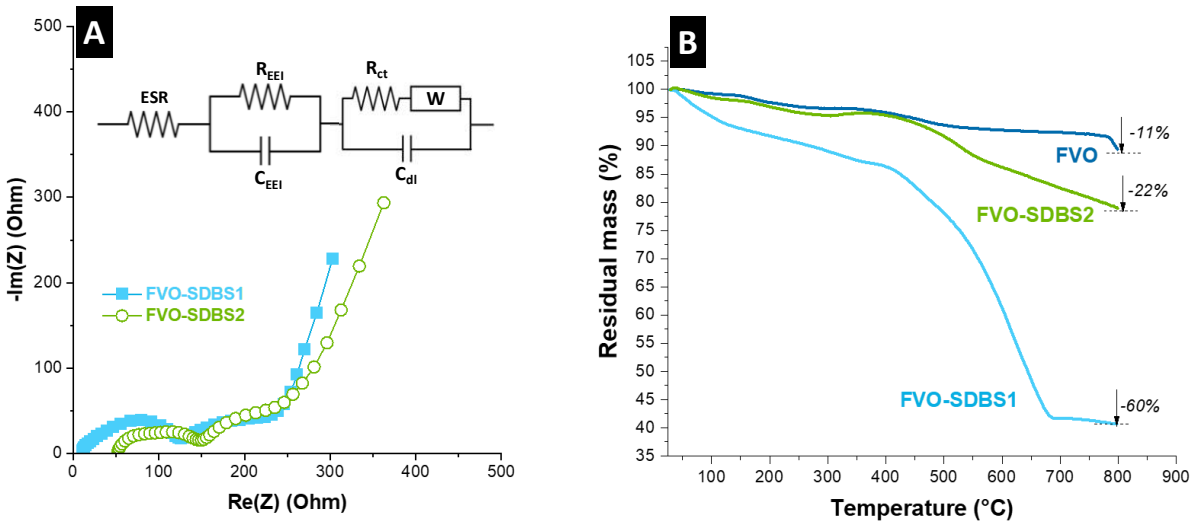

Figure S8. **A** Nyquist plot of FVO-SDBS1 and FVO-SDBS2. The inset shows the corresponding EIS equivalent circuit. **B** TGA curves of FVO, FVO-SDBS1, and FVO-SDBS2 under Ar.

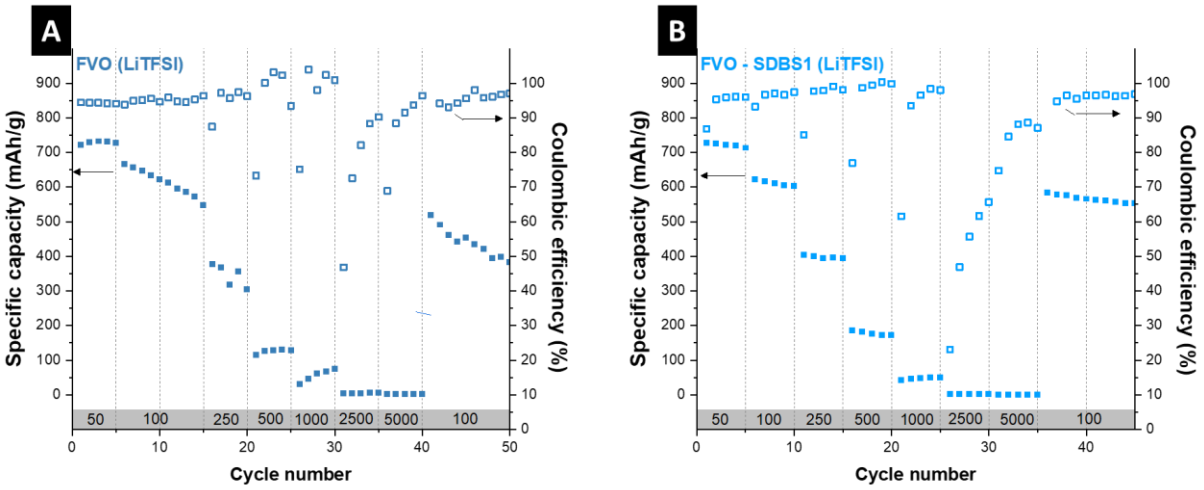

Figure S9. Galvanostatic charge/discharge cycling at 50-5000 mA/g for **A** FVO and **B** FVO-SDBS1.

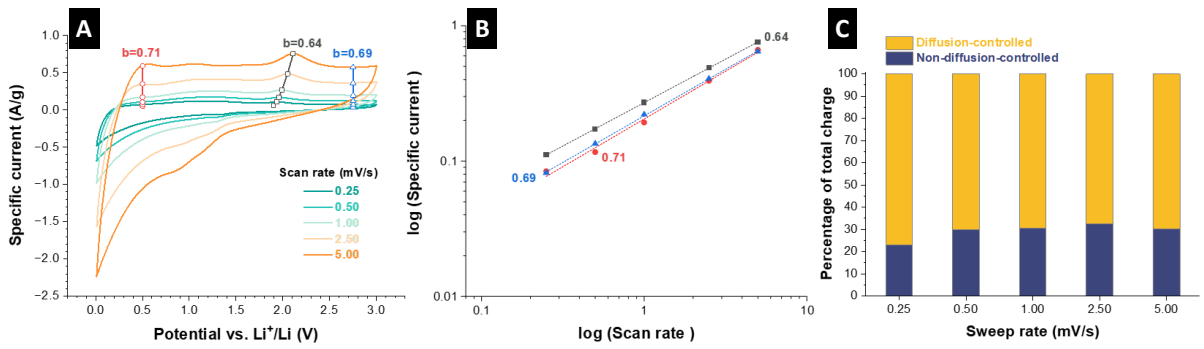

Figure S10. Cyclic voltammetry of FVO-SDBS1 at scan rates of 0.25-5.00 mV/s with their respective b-values at different potentials. **B** Specific current vs. scan rate at the maximum potential of each cycle, as well as potentials 0.5 V vs. Li/Li^+ and 2.75 V vs. Li/Li^+. **C** Calculated charge storage percentage from diffusion-controlled and non-diffusion-controlled charge from k_1 and k_2 values at different scan rates.

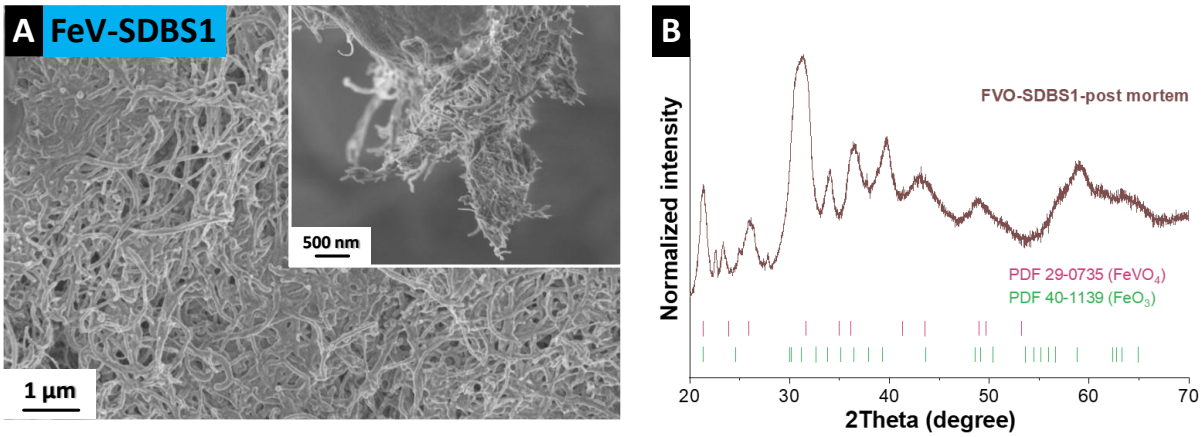

Figure S11. Post-mortem analysis of FVO-SDBS1. **A** Scanning electron micrograph of the electrode surface and **B** X-ray diffractogram of the electrode.

Table S1. Equivalent series resistance (ESR), the resistance of the electrode-electrolyte interphase (R_{EEI}), charge transfer resistance (R_{ct}), and Warburg resistance (R_W) of the tested cells.

Materials	ESR (Ω)	R_{EEI} (Ω)	R_{ct} (Ω)	R_w (Ω)
FVO-SDBS1	10.8	66.1	177.5	219.8
FVO-SDBS2	52.3	103.2	207.6	227.7